# Improving Inertial Velocity Estimation Through Magnetic Field Gradient-based Extended Kalman Filter

Makia Zmitri, Hassen Fourati, Christophe Prieur

# Improving Inertial Velocity Estimation Through Magnetic Field Gradient-based Extended Kalman Filter

Makia Zmitri
*Univ. Grenoble Alpes*
*CNRS, Grenoble INP, GIPSA-lab*
Grenoble, France
makia.zmitri@gipsa-lab.fr

Hassen Fourati
*Univ. Grenoble Alpes*
*CNRS, Grenoble INP, GIPSA-lab, Inria*
Grenoble, France
hassen.fourati@gipsa-lab.fr

Christophe Prieur
*Univ. Grenoble Alpes*
*CNRS, Grenoble INP, GIPSA-lab*
Grenoble, France
christophe.prieur@gipsa-lab.fr

***Abstract*—In this paper we focus on the velocity estimation problem of a rigid body and how to improve it with magneto-inertial sensors-based theory. We provide a continuous-time model that describes the motion of the body and we augment it after by introducing a new magnetic field gradient equation instead of using its value directly as an input for the model, as done usually in the corresponding literature. We investigate the advantage of moving to higher order spatial derivatives of the magnetic field in the estimation of velocity. These derivatives are computed thanks to a determined arrangement of magnetometers array. Within this framework, a specific set configuration of Extended Kalman Filters (EKFs) is proposed to focus mainly on the estimation of velocity and attitude of the body, but includes also an estimation of the magnetic field and its gradient. Some simulations for a specific scenario are proposed to show the improvements that we bring to the velocity estimation.**

***Index Terms*—Magnetic field gradient, spatial derivatives, velocity and attitude estimation, quaternion, EKF.**

## I. Introduction

In the last few years, indoor positioning has become an interest of many researchers as it brings a new challenge to the navigation field, especially with the unavailability of GPS information. However, a wide range of the proposed solutions to this problem requires a heavy infrastructure to work (Wireless Local Area Network (WLAN) [1], Radio Frequency Identification (RFID) [2], etc.), whereas others rely on optical [3] or multi-sensors [4], which can be inaccessible in certain applications that have cost and time constraints. More advanced and smart ways to get a velocity/position information have thus to be explored.

Inertial Measurement Units (IMUs), composed of inertial and magnetic sensors, have provided a promising solution for many of the encountered systems. Nevertheless, their huge drifts introduce another problem that needs to be treated with care. Some techniques have been proposed in literature to deal with these drawbacks. Some of them depend on foot-mounted dead reckoning method [5] which allows positioning in unknown environments by using the Zero-Velocity Update technique (ZUPT) in [6] and [7], for example. Other works exploit information about the structure of the building, namely by applying Heuristic Drift Elimination (HDE) method [8]. Others use magnetic fingerprinting in the purpose of identifying heading [9], by exploring the geomagnetic field anomalies. Yet, this requires the magnetic field to be mapped beforehand. In addition, the magnetic field presents high disturbances in indoor environment, which is considered as a sufficient argument for ignoring it entirely as a source of heading information. The large disturbances of the magnetic field that are observed in buildings (typically yielding $30^\circ$ of heading error) may generate significant misinterpretations in the determination of position. However, these disturbances are not in fact a simple random noise, on the contrary they are structured by physics equations, for instance, Maxwell's equations [10] that represent the propagation of electromagnetic phenomena. The disturbances are due to all the metals used in buildings (door frames, Aluminum windows, etc.) and potentially to the strong electric currents propagating close-by. Therefore rich information lies in those disturbances. Based on these phenomena, magneto-inertial approaches are proposed recently in [11], [12], [13], [14] with different dynamic models. They preserve the main advantages of purely inertial technology: no prior mapping and signal are required. In these works, the magnetic field gradient is considered as a known input for the state-space model. This gradient is usually noisy and is subject to singularities. This influences negatively the estimation process and observability and leads to estimation errors. Contrarily in [15], the authors considered that measurements of the magnetic field gradient are not available, instead the gradient is moved to the state vector and is estimated by an observer. Nevertheless, the dynamic of this gradient is modeled with a white noise, which is a questionable choice in our knowledge. In this paper, we focused on how to improve velocity estimation starting from the same technique as in [15]. The proposed approach takes advantage of the magnetic disturbances, by using a set of spatially distributed magnetometers to monitor the magnetic field and its spatial derivatives (gradient and its first derivative). The state-space model we considered in this work includes magnetic field gradient equation to describe its dynamic. A specific configuration of EKFs-based observer, to avoid some

nonlinearity issues, is proposed to estimate the velocity and eventually attitude of a rigid body in a magnetically disturbed environment, from a 3-axis magnetometers array, 3-axis gyroscope and 3-axis accelerometer. The proposed approach includes also the estimation of magnetic field and its gradient, which represents the main novelty to improve the velocity estimation. Simulation results show a notable improvement on velocity estimation compared to when the magnetic field gradient is employed directly as a noisy filter input. Improving velocity accuracy will be useful to reduce greatly the drifts of an inertial navigation technique, i.e. the position determination. This paper is organized as follows. In Section II we introduce some preliminaries and notations and we state the principle of the magneto-inertial navigation problem, then we reveal how the magnetic field gradient dynamic equation is established. An EKFs-based observer is designed in Section III, where the gradient equation is added, to tackle measurement noises and to estimate not only the velocity but also the attitude, the magnetic field and its gradient. Section IV presents some numerical simulations and displays the obtained results. While in Section V, we state some conclusions and potential future work.

## II. Problem statement

We consider the problem of velocity and attitude estimation of a rigid body using strapdown MEMS inertial sensors (composed of a triaxial gyroscope and accelerometer) and a spatially distributed triaxial magnetometer's array (a set of gradiometers). Especially, we focused on how to improve velocity estimation of a rigid body located inside a magnetically disturbed area, through exploring spatial derivatives of the magnetic field, starting from the same technique as in [15]. The proposed EKFs-based observer includes also the estimation of the attitude, magnetic field and its gradient.

### A. Preliminaries and notation

Let $\Re_n$ be an inertial frame and $\Re_b$ a body frame moving with the rigid body. Coordinates of vectors in $\Re_n$ (resp. $\Re_b$) are denoted with the prescript $n$ (resp. $b$).
Denote $R_{b\leftarrow n}$ the rotation matrix between these two frames, from $\Re_n$ to $\Re_b$. Since $R_{b\leftarrow n} \in SO(3)$, we have $R_{b\leftarrow n}^{-1} = R_{b\leftarrow n}^{\top}$.
We can represent $R_{b\leftarrow n}$ with unit quaternion $q = [q_0 \;\; q_1 \;\; q_2 \;\; q_3]^{\top} \in \mathbb{R}^{4\times 1}$ in the following way,

$$R_{b\leftarrow n} = \begin{bmatrix} 2(q_0^2+q_1^2)-1 & 2(q_1q_2+q_0q_3) & 2(q_1q_3-q_0q_2) \\ 2(q_1q_2-q_0q_3) & 2(q_0^2+q_2^2)-1 & 2(q_0q_1+q_2q_3) \\ 2(q_0q_2+q_1q_3) & 2(q_2q_3-q_0q_1) & 2(q_0^2+q_3^2)-1 \end{bmatrix} \quad (1)$$

where values of $q_{0\leq i\leq 3}$ are real and are between $-1$ and 1. More details about quaternion algebra can be found in [16].
We omitted in the rest of the paper the notation $R_{b\leftarrow n}$ for a simplicity reason and we used rather $R$.
We denote $\omega^{\frac{b}{n}} = [\omega_x \;\; \omega_y \;\; \omega_z]^{\top} \in \mathbb{R}^{3\times 1}$, the angular velocity of $\Re_b$ with respect to $\Re_n$, that is measured by a triaxial gyroscope. We can define its skew-symmetric matrix such as,

$$[\omega^{\frac{b}{n}}\times] = \begin{pmatrix} 0 & -\omega_z & \omega_y \\ \omega_z & 0 & -\omega_x \\ -\omega_y & \omega_x & 0 \end{pmatrix} \quad (2)$$

The well-known kinematic equation can be used to describe the variation of attitude in terms of quaternion [17] and [18],

$$\frac{dq}{dt} = \frac{1}{2}[\omega_q\times]q = \frac{1}{2}\begin{pmatrix} 0 & -\omega_x & -\omega_y & -\omega_z \\ \omega_x & 0 & \omega_z & -\omega_y \\ \omega_y & -\omega_z & 0 & \omega_x \\ \omega_z & \omega_y & -\omega_x & 0 \end{pmatrix} q \quad (3)$$

where $\omega_q = [0 \;\; \omega_x \;\; \omega_y \;\; \omega_z]^{\top} \in \mathbb{R}^{4\times 1}$ and $[\omega_q\times]$ is its skew-symmetric matrix.
The rigid body under consideration can simultaneously translate and rotate in 3D space. Let $P_b = [x_p \;\; y_p \;\; z_p]^{\top} \in \mathbb{R}^{3\times 1}$ denote the sensor board point of percussion, which is a fixed point in $\Re_b$. The trajectory of $P_b$ can be represented by the position vector $M_n = [x_m \;\; y_m \;\; z_m]^{\top} \in \mathbb{R}^{3\times 1}$ in $\Re_n$, such as we have,

$$M_n = R^{\top}P_b + D_n \quad (4)$$

where $D_n = [D_{nx} \;\; D_{ny} \;\; D_{nz}]^{\top} \in \mathbb{R}^{3\times 1}$ stands for the displacement (translation) of the rigid body in $\Re_n$.
Let $v_n = \frac{dM_n}{dt} = [v_{nx} \;\; v_{ny} \;\; v_{nz}]^{\top} \in \mathbb{R}^{3\times 1}$ be the velocity vector of $M_n$ in $\Re_n$, and $a_n = \frac{dv_n}{dt} = [a_{nx} \;\; a_{ny} \;\; a_{nz}]^{\top} \in \mathbb{R}^{3\times 1}$ the associated acceleration vector.
The vectors $v_n$ and $a_n$ can also be expressed in body frame using the following multiplication by $R$,

$$v_b = Rv_n \quad (5)$$

and,

$$a_b = Ra_n \quad (6)$$

We denote $B_b = [B_{bx} \;\; B_{by} \;\; B_{bz}]^{\top} \in \mathbb{R}^{3\times 1}$ the magnetic field in $\Re_b$, which depends on time and space. The theoretical expression of a triaxial magnetometer output attached to a rigid body can be modeled by,

$$B_b = RB_n \quad (7)$$

where $B_n = [B_{nx} \;\; B_{ny} \;\; B_{nz}]^{\top} \in \mathbb{R}^{3\times 1}$ is the Earth's magnetic field expressed in $\Re_n$.
The components of $B_n$ can be determined using the World Magnetic Model (WMM) online calculator [19].
The Jacobian matrix of the magnetic field at $P_b$ is defined as,

$$\nabla B_b(P_b(t)) = \frac{\partial B_b(P_b(t))}{\partial P_b(t)} \quad (8)$$

This Jacobian represents the magnetic field gradient and can be described with the following matrix,

$$\nabla B_b = \begin{bmatrix} \frac{\partial B_{bx}}{\partial x_p} & \frac{\partial B_{by}}{\partial x_p} & \frac{\partial B_{bz}}{\partial x_p} \\ \frac{\partial B_{bx}}{\partial y_p} & \frac{\partial B_{by}}{\partial y_p} & \frac{\partial B_{bz}}{\partial y_p} \\ \frac{\partial B_{bx}}{\partial z_p} & \frac{\partial B_{by}}{\partial z_p} & \frac{\partial B_{bz}}{\partial z_p} \end{bmatrix} = (\alpha_{ij})_{1\leq i,j\leq 3} \quad (9)$$

According to Maxwell's equations [10], the Earth's magnetic field in $\Re_b$ satisfies the following evolution equation[1],

$$\frac{dB_b}{dt} = -\omega^{\frac{b}{n}} \times B_b + \nabla B_b v_b \tag{10}$$

As long as $\nabla B_b$ is non-singular, we can observe and reconstruct the velocity vector $v_b$ (see [15] for observability proof).

### *B. Higher order spatial derivatives of magnetic field*

A set of spatially distributed magnetometers can deliver two measurements. First, this set gives $B_b$ in $\Re_b$, measured by each sensor. Then, using the data provided by the set of sensors, $\nabla B_b$ can be determined by a finite difference scheme.
If higher order spatial derivatives are measurable (see [20]), an improvement on velocity estimation can be achieved by exploiting the following equation,

$$\frac{d\nabla B_b(P_b(t))}{dt} = f(\frac{\partial \nabla B_b(P_b(t))}{\partial P_b(t)}, v_b) \tag{11}$$

For that, we first introduce the temporal derivative of the magnetic field gradient in $\Re_n$ such as,

$$\frac{d\nabla B_n}{dt} = \frac{d\nabla B_n}{dM_n}\frac{dM_n}{dt} = T_n v_n \tag{12}$$

where $T_n \in \mathbb{R}^{3\times3\times3}$ is a tensor representing the first spatial derivative of the magnetic field gradient in $\Re_n$.

$$T_n = \frac{d\nabla B_n}{dM_n} = \begin{bmatrix} \nabla\alpha_{11} & \nabla\alpha_{12} & \nabla\alpha_{13} \\ \nabla\alpha_{21} & \nabla\alpha_{22} & \nabla\alpha_{23} \\ \nabla\alpha_{31} & \nabla\alpha_{32} & \nabla\alpha_{33} \end{bmatrix} \tag{13}$$

and $\nabla\alpha_{ij} = [\frac{\partial\alpha_{ij}}{\partial x_m} \quad \frac{\partial\alpha_{ij}}{\partial y_m} \quad \frac{\partial\alpha_{ij}}{\partial z_m}]_{1\le i,j\le 3}$.
As all measurements from the magnetometer array are acquired in $\Re_b$, we must write (12) in $\Re_b$ rather than $\Re_n$. Thus, we have,
$\frac{d\nabla B_n}{dt} =$

$$\begin{aligned}\frac{d(R\nabla B_b R^\top)}{dt} &= \frac{dR}{dt}\nabla B_b R^\top + R\frac{d\nabla B_b}{dt}R^\top + R\nabla B_b\frac{dR^\top}{dt} \\ &= R[\omega^{\frac{b}{n}}\times]\nabla B_b R^\top + R\frac{d\nabla B_b}{dt}R^\top + R\nabla B_b(-[\omega^{\frac{b}{n}}\times]R^\top) \\ &= T_n v_n \end{aligned} \tag{14}$$

In $\Re_b$ we obtain then,

$$R\frac{d\nabla B_b}{dt}R^\top = T_n v_n + R\nabla B_b[\omega^{\frac{b}{n}}\times]R^\top - R[\omega^{\frac{b}{n}}\times]\nabla B_b R^\top \tag{15}$$

By multiplying both sides of (15) by $R^\top$ and $R$ respectively, we deduce the following equation,

$$\frac{d\nabla B_b}{dt} = T_b v_b + \nabla B_b[\omega^{\frac{b}{n}}\times] - [\omega^{\frac{b}{n}}\times]\nabla B_b \tag{16}$$

where $T_b$ is the first spatial derivative of the magnetic field gradient, with the same form as (13), represented in $\Re_b$. If the magnetic field is assumed to satisfy Maxwell's equations for a source-free region of space, then $\nabla B_b$ can be described with only 5 degrees of freedom. Maxwell's equations imply that the magnetic field gradient is symmetric and traceless,

$$\begin{cases} \partial_1 B_{b1} + \partial_2 B_{b2} + \partial_3 B_{b3} &= 0 \\ \forall\ \ i,j \in \{1,2,3\}, \quad \partial_i B_{bj} &= \partial_j B_{bi} \end{cases} \tag{17}$$

Therefore, the third column of $\nabla B_b$ in (9) can be recovered from the first two columns. In other words, a 2 dimensional arrangement of sensors is sufficient to recover the full magnetic field gradient and its first spatial derivative.
Variations of the magnetic field on a small scale may not be easily measured, so the finite difference scheme can be inapplicable. One possibility to address this problem is to use the higher order spatial interpolation of the magnetic field. Yet, one might wonder if this interpolation is achievable using a planar arrangement of sensors. For this reason, we introduce the following two Lemmas, demonstrated in [11]. Assuming that all components of the magnetic field are of class $C^n$ (i.e. $n$ times differentiable and its $n$-th derivative is continuous). On the basis of (17) and thanks to Schwarz's theorem [21], the following Lemma holds,

*Lemma 1.* Let $\rho$ be a function from {1,2,...,n} to {1,2,3}. For any permutation $\sigma$ on {1,2,...,n}, with $n > 1$, we have,
$\partial_{\rho(1)}\partial_{\rho(2)}...\partial_{\rho(n-1)}B_{b\rho(n)} =$

$$\partial_{\rho(\sigma(1))}\partial_{\rho(\sigma(2))}...\partial_{\rho(\sigma(n-1))}B_{b\rho(\sigma(n))} \tag{18}$$

Using the lemma above and (17), the following lemma holds,
*Lemma 2.* Expressions of the form $\partial_{\rho(1)}\partial_{\rho(2)}...\partial_{\rho(n-1)}B_{b\rho(n)}$ with $\rho$ be a function from {1,2,...,n} to {1,2,3}, can be represented as a linear combination of these terms, such that any of them admits at most one index equal to 3.

Accordingly, both these lemmas suggest that knowing spatial derivatives to order $n$ only along the first two spatial coordinates, with a planar arrangements of magnetometers, is enough to deduce all the rest of spatial derivatives of order $n$. Then, we can identify then the number of sensors needed to compute these spatial derivatives by exploiting different second derivative calculus theorems and approximations (Taylor series, Schwarz's theorem, etc.). We have been able to effectively compute the second derivative of the magnetic field with the optimal number of magnetometers. For that, we only estimate $\alpha_{11}$, $\alpha_{12}$, $\alpha_{13}$, $\alpha_{22}$, and $\alpha_{23}$, which correspond respectively to $\frac{\partial B_{bx}}{\partial x_p}$, $\frac{\partial B_{by}}{\partial x_p}$, $\frac{\partial B_{bz}}{\partial x_p}$, $\frac{\partial B_{by}}{\partial y_p}$ and $\frac{\partial B_{bz}}{\partial y_p}$ in (9), while the rest of elements of the magnetic field gradient are deduced using (17). As for $T_b$, we need to measure only 8 from the 27 elements of this tensor, that are $\frac{\partial^2 B_{bx}}{\partial x_p^2}$, $\frac{\partial^2 B_{bx}}{\partial y_p \partial x_p}$, $\frac{\partial^2 B_{by}}{\partial x_p^2}$, $\frac{\partial^2 B_{by}}{\partial y_p^2}$, $\frac{\partial^2 B_{by}}{\partial y_p \partial x_p}$, $\frac{\partial^2 B_{bz}}{\partial x_p^2}$, $\frac{\partial^2 B_{bz}}{\partial y_p^2}$ and $\frac{\partial^2 B_{bz}}{\partial y_p \partial x_p}$, while we deduce the other elements from (17).

## III. Design of the EKFs-based observer

In this section, we focused mainly on inertial velocity estimation and how to improve it according to the literature. A specific configuration of EKFs-based observer is proposed based on a 3-axis magnetometers array, 3-axis gyroscope and

[1] $\times$ is the cross product of two vectors in $\mathbb{R}^3$.

3-axis accelerometer. The proposed approach includes also the estimation of attitude, magnetic field and its gradient, which represents the main novelty to improve the velocity estimation. A discrete-time dynamic model and measurement one are provided in a first step, based on the considered continuous-time models.

### A. Continuous-time dynamic and measurement models

The continuous-time dynamic model used to establish the EKFs-based observer can be written such as,

$$\begin{cases} \dfrac{dq}{dt} = \dfrac{1}{2}\begin{bmatrix} -q_i^\top \\ I_{3\times3}q_0 + [q_i\times] \end{bmatrix}_{1\le i\le 3} \omega^{\frac{b}{n}} \\ \dfrac{dv_b}{dt} = -\omega^{\frac{b}{n}} \times v_b + a_b \\ \dfrac{dB_b}{dt} = -\omega^{\frac{b}{n}} \times B_b + \nabla B_b v_b \end{cases} \tag{19}$$

The state vector for this dynamic model is $x = [q \;\; v_b \;\; B_b]^\top \in \mathbb{R}^{10\times1}$ , the input vector is $u = [\omega^{\frac{b}{n}} \;\; a_b \;\; \nabla B_b]^\top \in \mathbb{R}^{11\times1}$, and the output (measurement) vector is $y = [a_b \;\; B_b]^\top \in \mathbb{R}^{6\times1}$. This model is proven observable in [11], and by computing the observability matrix $O$, we have $rank[O] = n$, with $n = 10$ is the number of the states of the dynamic model.

The magnetic field measurements are usually noisy, then in the process of extracting higher order derivatives, this noise can get more important, with the addition of uncertainties that come from the different approximations taken into consideration to compute the higher order derivatives. It follows that the magnetic field gradient $\nabla B_b$ will also be affected by noise. This can cause unbounded velocity estimation errors especially when the magnetic field gradient have low values (More precised simulations on the matter are in [11]). For this reason, estimating/filtering $\nabla B_b$ instead of using it directly as an input in the EKFs-based observer will be of benefit to improve the velocity estimation. As the first spatial derivative $T_b$ (used in (16)) of the magnetic field gradient is measurable, we can add $\nabla B_b$ to the state vector.

One might think that adding (16) to the continuous-time model (19) is the best way to address this problem. However, we noticed that augmenting the state vector with 5 additional states (as deduced from (17)) implies higher error in the computation of Jacobians for the linearization process of the nonlinear model (19), and thus worse results for the estimation of velocity. We propose later a solution for this problem by estimating the magnetic field gradient $\nabla B_b$ separately in a primary EKF and then we feed the estimation result to the main EKF. The continuous-time model for this approach is represented in Fig. 1.

### B. Discrete-time dynamic model

The discrete-time dynamic and measurement models, with Gaussian noises can be represented as following,

$$\begin{aligned} x[k] &= f(x[k-1], u[k], \eta[k]) \\ z[k] &= h(x[k], u[k], \nu[k]) \end{aligned} \tag{20}$$

where $x[k]$ is the state vector at time step $k$, $z[k]$ is the measurement vector, $u[k]$ is the input, $f(.)$ is a nonlinear function

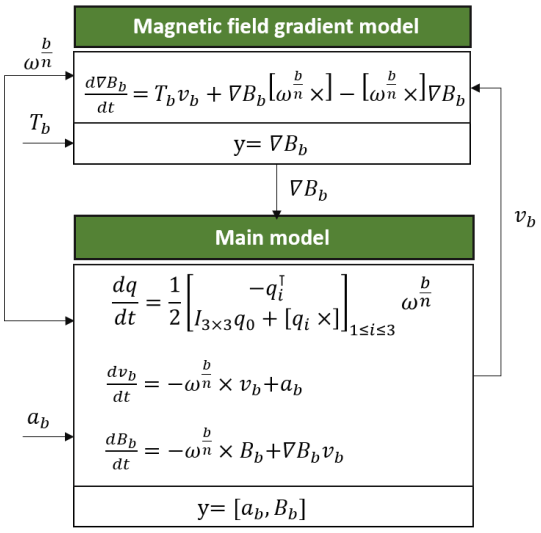


Fig. 1. Proposed model design

that represents the state-space model, $h(.)$ is a nonlinear function that represents the measurement model, and $\eta[k]$ and $\nu[k]$ are the process and measurement noises, respectively, and are assumed to be zero-mean, white, Gaussian and uncorrelated. The discretization is done through Euler approximation.

We explicit, for example, the discrete-time magnetic field dynamic equation, in order to better understand the effect of gradient noise on velocity estimation. The rest of the discrete-time dynamic model equations follow the same discretization principle and are not stated here. We have then,

$$B_b[k+1] = B_b[k] + T\alpha + T(\nabla B_b[k] + \eta_{\nabla B_b}[k])v_b[k] \tag{21}$$

where $T$ is the sampling time, $\alpha = (-w^{\frac{b}{n}}[k] + \eta_\omega[k]) \times B_b[k]$, and $\eta_{\nabla B_b}[k]$, $\eta_\omega[k]$ are the magnetic field gradient and the angular velocity noises, respectively. We remark that the noise term $\eta_{\nabla B_b}[k]$ is multiplied by the velocity $v_b[k]$. This justifies again the need to consider filtering the magnetic field gradient $\nabla B_b$ before feeding it to the main EKF.

### C. EKFs-based observer implementation

In the literature, it was shown that the EKF uses a two-step predictor-corrector algorithm [22]. First, it projects both the most recent state and the error covariance estimates, from a previous time, forwards in time, in order to compute a predicted (or a priori) estimate of the states at the current time. Next, we correct the predicted state in the first step by incorporating the last process measurements to generate an updated (or a posteriori) state and covariance estimates.

Yet, and because of the nonlinear nature of the system being estimated, the covariance prediction and update equations cannot use the state space model $f(.)$ and the measurement $h(.)$ directly, but instead, the Jacobians of these functions need

to be computed. They are defined as,

$$\begin{aligned} F_k =& \frac{\partial f}{\partial x}|_{\hat{x}_{k-1|k-1},u_k} \\ H_k =& \frac{\partial h}{\partial x}|_{\hat{x}_{k|k-1}} \end{aligned} \tag{22}$$

To optimize the computation time and memory allocation, we calculate the Jacobians periodically instead of on each step, this provided us with nearly the same results on velocity estimation errors.
The prediction step is given by,

$$\begin{aligned} \hat{x}_{k|k-1} =& f(\hat{x}_{k-1|k-1}, u_k) \\ P_{k|k-1} =& F_k P_{k-1|k-1} F_k^\top + Q_k \end{aligned} \tag{23}$$

while in the update step we start by computing the Kalman gain,

$$K_k = P_{k|k-1} H_k^\top S_k^{-1} \tag{24}$$

Then, the correction step is done through updating the state and the covariance estimates,

$$\begin{aligned} \hat{x}_{k|k} =& \hat{x}_{k|k-1} + K_k(z_k - h(\hat{x}_{k|k-1})) \\ P_{k|k} =& (I - K_k H_k) P_{k|k-1} \end{aligned} \tag{25}$$

It is known that the EKF is not optimal. In fact, if the process model is inaccurate because of the use of Jacobians $F_k$ and $H_k$ for the linearization of the models (including (16) for magnetic field gradient), the EKF may diverge or lead to unsuitable estimates.
For this reason, we avoided augmenting the state vector of the main EKF (related to (19)), and chose to estimate the magnetic field gradient on a separate primary EKF (related to (16)), as shown in Fig. 2.

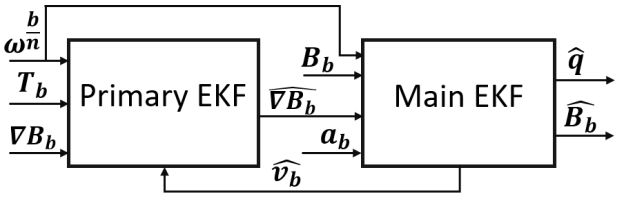


Fig. 2. EKFs-based observer design

## IV. Simulation results

### A. Preparing the framework for simulations

This section aims to illustrate the performance and accuracy of the designed EKFs-based observer. Some numerical simulations were carried out under MATLAB to estimate a rigid body velocity, attitude, magnetic field and its gradient, based on theoretical inertial and magnetic measurements. We consider an attitude variation example taken from angular velocity data over 200s. The following angular rate values are simulated,

$$\begin{cases} \omega_x = -1.8\ sin(1.5t) \\ \omega_y = 0.5\ cos(0.9t) \\ \omega_z = 1.5\ sin(1.2t) \end{cases} \tag{26}$$

where $t$ is the time varying until 200s. Then, the first kinematic equation in the dynamic model (19) is solved to obtain the continuous-time motion in quaternion using the angular velocity data in (26). The obtained quaternion is used as a reference to compare it with the estimated one from the proposed EKFs-based observer. The rotation matrix in (1) is then computed from the reference trajectory in quaternion coordinates. We simulate the sensor measurements $a_b$ and $B_b$ using (4), (6), (7) and the rotation matrix computed from the reference quaternion. We calculate also the magnetic field gradient and its derivative using Taylor approximations and Schwarz's theorem (see Lemmas 1 and 2). A realistic simulation needs to consider sensor noises and the impact of spatial discretization since the spatial gradient of the magnetic field $\nabla B_b$ in $\Re_b$ is not constant. To represent the sensor imperfections, an additive random zero-mean white Gaussian noise is considered for all measurements with a large standard deviation (see Table I).

TABLE I
Characteristics of the various noises for sensor measurements

| Sensors | Parameters | Standard deviations | Units |
|---|---|---|---|
| 3-axis accelerometer | $\eta_{a_b}$ | 0.1 | $\mathrm{ms}^{-2}$ |
| 3-axis gyroscope | $\eta_\omega$ | 0.05 | $\mathrm{rads}^{-1}$ |
| 3-axis magnetometer | $\eta_{B_b}$ | 0.1 | G |

The process and the measurement covariances $R_{EKF}$ and $Q_{EKF}$, respectively, are set according to the considered sensor noise levels . In the proposed simulation, the dynamic model and the EKFs-based observer are initialized with different conditions. Notice that this choice allows us to illustrate the convergence of the two estimators (primary and main) even though it was initialized far from the actual states of the model.

### B. Results

We have used Monte-Carlo simulation technique to run the algorithm for 100 times. This is done to give more precise results as we employ randomness in the noises generation and then mean-squared error values can change from one code execution to another under MATLAB. The EKFs-based observer uses the acceleration and the magnetic field to compensate for the slowly increasing drift from the time integral of angular velocity (see [23] for a detailed explanation). Fig. 3 shows the estimation error of the quaternion components for the first 10s of the simulation time interval (for figure clarity purposes). Note that the estimated quaternion components converge in less than 2s despite initializing the main EKF far from the theoretical quaternion scenario. By using (16) and (17), we estimated 5 elements of the magnetic field gradient $\nabla B_b$ and deduced the other 4 elements. Fig. 4 displays the estimation results for the magnetic field gradient. Note that the estimated gradient (in blue dashed line) is very close to the theoretical one (in red solid line). We note that the initialization was different as for the quaternion. This is clearly an advantage as employing the estimated gradient instead of the noisy one (in

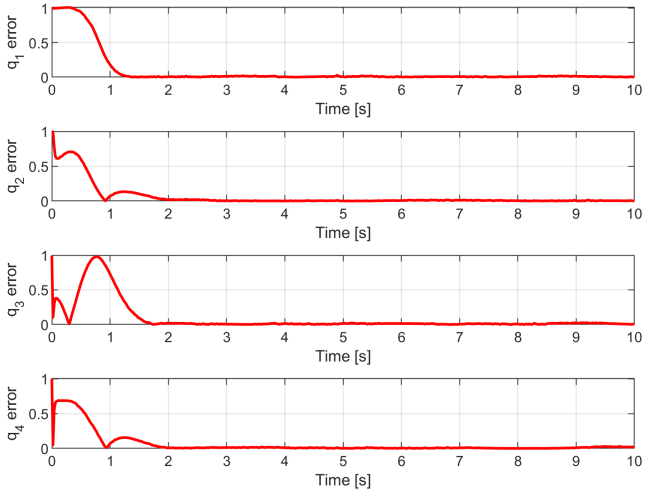


Fig. 3. Estimation error on the quaternion components

green solid line) will later improve the velocity estimation. The mean-squared error (MSE), between the theoretical gradient elements and those estimated is in the order of 3. $10^{-4}$G.

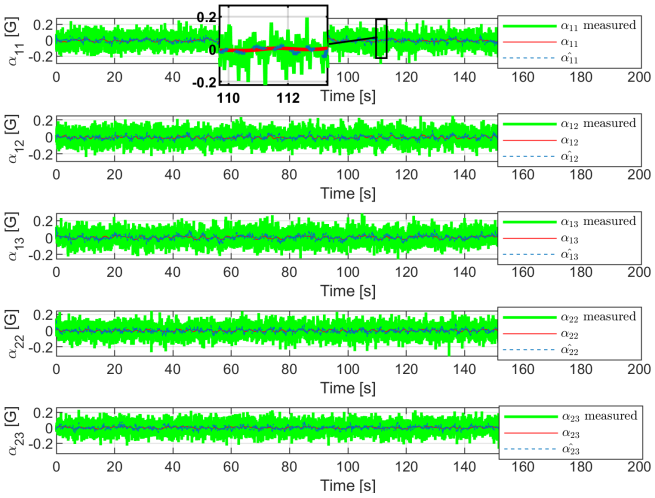


Fig. 4. Magnetic field gradient estimation

We also see in Fig. 5 that the estimated magnetic field converges to the theoretical one despite the high standard deviation considered on its measurements, with a mean-squared error around $10^{-3}$G (initialization was different as for the quaternion).

Fig. 6 shows the result of velocity estimation, where we can observe that the convergence (with different initialization) is obtained after few seconds with a small error due to the different uncertainties considered in the simulation scenario, i.e. the approximations taken into account to extract the spatial derivatives, the linearization process of the two EKFs, etc.

Table II displays the MSE for the velocity estimation with the implementation of the primary EKF for the magnetic field gradient estimation and without (the magnetic field gradient is used as a noisy input). The MSE has clearly decreased which

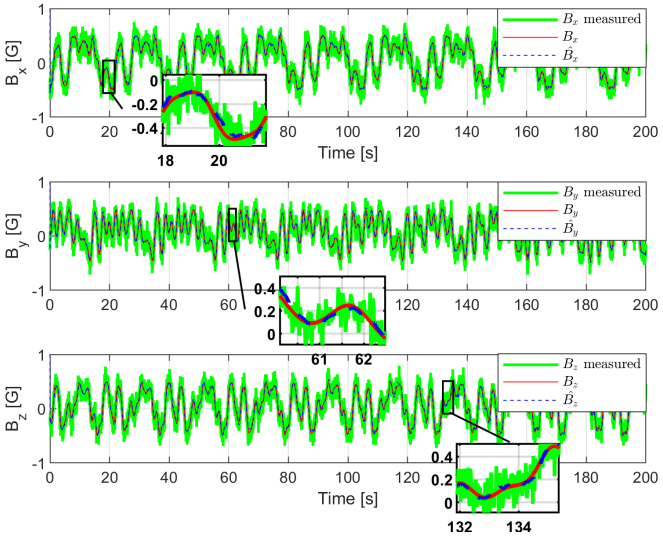


Fig. 5. Magnetic field estimation

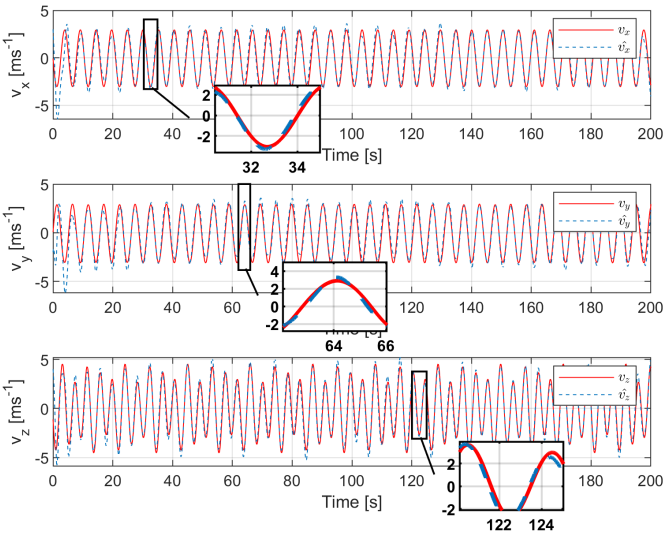


Fig. 6. Velocity estimation

is a very promising contribution in the future to better estimate the position.

TABLE II
MSE OF VELOCITY ESTIMATION

| Primary EKF | *Without* | *With* |
|---|---|---|
| Velocity MSE ($\mathrm{ms}^{-1}$) | 0.49 | 0.29 |

The same results can be outlined in Fig. 7 by computing the cumulative distribution function [24] in both cases (with and without the primary EKF). Fig. 7 shows how the proposed approach provides better results, in terms of error between the theoretical velocity and the estimated one. For instance, without using the primary EKF, only 30% of $v_x$ estimation error is inferior to $0.5\mathrm{ms}^{-1}$, contrarily to 60% when applying the primary EKF.

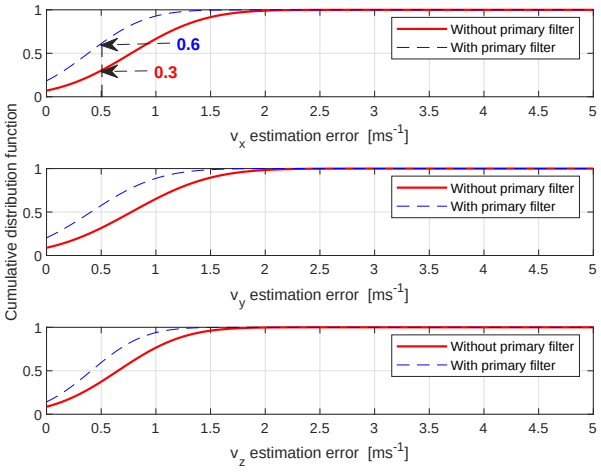


Fig. 7. Velocity estimation errors cumulative distribution function

## V. Conclusion and Future Work

In this paper, it was shown that the information lying in the disturbances of the magnetic field is reliable enough to provide a better velocity estimate. Higher order derivatives were computed from a set of spatially distributed magnetometers in order to represent the dynamic of the magnetic field gradient. By designing a primary EKF, the noise in the magnetic field gradient was reduced and consequently velocity estimation errors decreased with the main EKF filter. Attitude has also been reconstructed by providing acceleration/angular velocity measurements in the body frame along with the magnetic field. Applying this approach on real experimental data is definitely the next step. Different set of trajectories need also to be tested, mainly static trajectories (constant attitude, zero velocity) where inertial sensor biases can be hard to identify. Position drift coming from integrating velocity errors should also be examined, especially in the case of unknown initial position.

## References


[1] M. Ciurana, S. Cugno, and F. Barcelo-Arroyo, "WLAN Indoor Positioning Based on ToA with Two Reference Points," in 4th Workshop Positioning, Navigation and Communication, Hannover, Germany, 2007.

[2] A. A. N. Shirehjini, A. Yassine and S. Shirmohammadi, "An RFID-based position and orientation measurement system for mobile objects in intelligent environments," IEEE Trans. Instrum. Meas., vol. 61, no. 6, pp. 1664–1675, 2010.

[3] R. Mautz and S. Tilch. "Survey of optical indoor positioning systems," in International Conference on Indoor Positioning and Indoor Navigation (IPIN), pp. 1–7, Guimaraes, Portugal, 2011.

[4] J. Wu, Z. Zhou, H. Fourati, R. Li and M. Liu. "Generalized Linear Quaternion Complementary Filter for Attitude Estimation from Multi-Sensor Observations: An Optimization Approach," IEEE Transactions on Automation Science and Engineering, pp. 1–14, 2019.

[5] A. Makni, A. Kibangou and H. Fourati. "Data Fusion-Based Descriptor Approach for Attitude Estimation underaccelerated maneuvers," Asian Journal of Control, pp. 1–11, 2019.

[6] H. Fourati. "Heterogeneous data fusion algorithm for pedestrian navigation via foot-mounted inertial measurement unit and complementary filter," IEEE Transactions on Instrumentation and Measurement vol. 64, no. 1, pp. 221–229, 2015.

[7] I. Skog, J.-O. Nilsson, and P. Händel. "Evaluation of zero-velocity detectors for foot-mounted inertial navigation systems," in International Conference on Indoor Positioning and Indoor Navigation (IPIN)," pp. 1–6, Zurich, Switzerland, 2010.

[8] J. Borenstein and L. Ojeda, "Heuristic drift elimination for personnel tracking systems," Journal of Navigation, vol. 63, pp. 591–606, 2010.

[9] J. Chung, M. Donahoe, C. Schmandt, I.-J. Kim, P. Razavai, and M. Wiseman. "Indoor location sensing using geo-magnetism," in 9th international conference on Mobile systems, applications, and services (MobiSys), pp. 141–154, Washington DC, USA, 2011.

[10] J.D. Jackson. "Classical Electrodynamics," Third Edition. John Wiley & Sons, Inc.,1998.

[11] C.-I. Chesneau. "Magneto-Inertial Dead-Reckoning in inhomogeneous field and indoor applications," PhD thesis, Grenoble Alpes University, France 2018.

[12] C.-I. Chesneau, M. Hillion, J.-F. Hullo, G. Thibault and C. Prieur. "Improving magneto-inertial attitude and position estimation by means of a magnetic heading observer," in International Conference on Indoor Positioning and Indoor Navigation (IPIN), pp. 1–8, Sapporo, japon, 2017.

[13] C.-I. Chesneau, M. Hillion and C. Prieur. "Motion estimation of a rigid body with an EKF using magneto-inertial measurements," in International Conference on Indoor Positioning and Indoor Navigation (IPIN), pp. 1–6, Madrid, Spain, 2016.

[14] E. Dorveaux. "Magneto-inertial navigation: principles and application to an indoor pedometer," PhD thesis, Ecole Nationale Supérieure des Mines de Paris, France, 2011.

[15] D. Vissière, A.-P. Martin, and N. Petit. "Using spatially distributed magnetometers to increase IMU-based velocity estimation in perturbed areas," in 46th IEEE Conference on Decision and Control, New Orleans, Louisiana, USA, 2007.

[16] J. B. Kuipers. "Quaternions and rotation sequences," Vol. 66, 1999.

[17] Z. Zhang, Z. Zhou, J. Wu, S. Du and H. Fourati. "Fast Linear Attitude Estimation and Angular Rate Generation," in International Conference on Indoor Positioning and Indoor Navigation (IPIN), pp. 1–7, Nantes, France, 2018.

[18] T. Michel, P. Genevès, H. Fourati and N. Layaïda. "Attitude estimation for indoor navigation and augmented reality with smartphones," Pervasive and Mobile Computing, vol. 46, pp. 96–121, 2018.

[19] NOAA. "The world magnetic model," http://www.ngdc.noaa.gov, 2015.

[20] I. Skog, G. Hendeby, and F. Gustafsson. "Magnetic odometry - a model-based approach using a sensor array," in 21st International Conference on Information Fusion (FUSION), Cambridge, United Kingdom, 2018.

[21] R. G. D. Allen. "Mathematical Analysis for Economists," pp. 300–305, 1964.

[22] T. Kailath. "Lectures on Wiener and Kalman Filtering," 1981.

[23] H. Fourati, N. Manamanni, L. Afilal and Y. Handrich. "A Nonlinear Filtering Approach for the Attitude and Dynamic Body Acceleration Estimation Based on Inertial and Magnetic Sensors: Bio-Logging Application," IEEE Sensors Journal, vol. 11, no. 1, pp. 233–244, 2011.

[24] N. A. J. Hastings and J. B. Peacock. "Statistical Distributions," 1975.